

Electronic transmission properties in a mesoscopic necklace with inhomogeneous magnetic flux

Zhiwen Pan

National Key Laboratory of Solid State Microstructures and Department of Physics, Nanjing University, Nanjing 210093, China

Chang-De Gong

CCAST (World Laboratory), P.O. Box 8730, Beijing 100080, China
and Department of Physics, Nanjing University, Nanjing 210093, China

Mak Hon Lung and Haiqing Lin

Department of Physics, The Chinese University of Hong Kong, Shatin, Hong Kong, China

(Received 4 September 1998)

The electronic transmission properties and the energy spectrum of a mesoscopic necklace with inhomogeneous flux is calculated. We found interesting transmission behavior that is quite different from the case with homogenous flux. In this model, the transmission depends on both the modulation mode and the amplitude of the flux. The electronic transmission properties can be explained from the energy spectrum of the system. [S1063-651X(99)05904-8]

PACS number(s): 52.35.Mw, 73.23.-b, 72.10.-d

I. INTRODUCTION

Quantum transport through mesoscopic systems has been extensively studied during recent years [1–10]. With the development of fabrication technology in semiconductors and related areas, it is possible to fabricate devices with size smaller than the electronic coherence length and thus electrons can tunnel through the samples coherently and show some interesting quantum mechanical effects, such as persistent current in isolated mesoscopic rings [5], etc. This may open a very rich field of great theoretical and experimental interest concerning these devices.

For the mesoscopic systems, theoretical study has largely concentrated on the persistent current of isolated rings [5,6,11] and the transmission of electrons through open ring systems that are connected via leads to electron reservoirs [12–16]. In both cases, the rings are threaded by a magnetic flux Φ .

Recently, Takai and Ohta investigated the quantum oscillation and Aharonov-Bohm effect in a multiply connected normal-conductor loop [17,18] and obtained many interesting results. In their systems, rings are serially connected via a lead between two succeeding rings. These authors have all considered the case of the mesoscopic system with homogenous flux. However, it is interesting to ask what will happen if the systems are threaded by an inhomogeneous flux. Theoretically speaking, since the energy spectrum of the electrons in this case will definitely differ from the case with constant magnetic flux, and thus will cause some changes in the electronic transmission properties, the changes could lead to certain transmission properties that would then be available to examine the predictions of the quantum interference effect. Experimentally speaking, it is now possible to construct and detect the field inhomogeneous at the scale of deep sub- μm , thus providing the possibility of examining it; and these new transmission properties will perhaps be useful for designing a new type of device. In the case with inhomogeneous magnetic flux, neighboring rings will carry different

flux, i.e., the hopping integral in each ring will be modulated by a different phase, and therefore results in some mismatches of phase between neighboring rings, thus leading to certain interference effects. In this paper we will investigate the electronic transmission properties of a mesoscopic open necklace of loop geometry [19,20] with inhomogeneous flux. The structure of it is illustrated in Fig. 1. This structure is similar to that of Takai and Ohta but differs from theirs in terms of which of the succeeding rings in this model are directly connected.

The Hamiltonian of the system can be written as

$$H = \sum_i \epsilon_i c_i^\dagger c_i + \sum_{\langle i,j \rangle} V_{i,j} c_i^\dagger c_j, \quad (1)$$

where the c_i^\dagger (c_i) is the creation (annihilation) operator, and ϵ_i is the on-site energy, which is set to be 0 in this paper. $V_{i,j}$ is the nearest-neighbor overlap integral, which is modulated by the magnetic flux, and can be written as $V_{i,j} = V e^{i\theta_{ij}}$, where θ_{ij} is the phase imposed by the magnetic field on the hopping from site i to site j , V is the intrinsic overlap integral and it is set to be 1 as a unit of energy in this paper.

It is easy to write the following equations for the wave amplitudes on the upper arm, the lower arm, and the necklace nodes as

$$E \varphi_n = e^{-i\gamma_{n-1}/4} \chi_{n-1} + e^{i\gamma_{n-1}/4} \psi_{n-1} + e^{i\gamma_n/4} \chi_n + e^{-i\gamma_n/4} \psi_n, \quad (2)$$

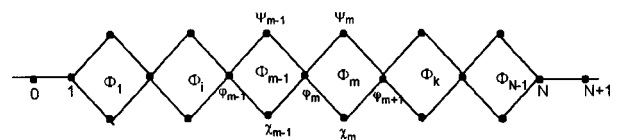


FIG. 1. The necklace with inhomogeneous flux. Each loop is threaded by a different flux Φ_i , and the system is connected to two semi-infinite linear leads.

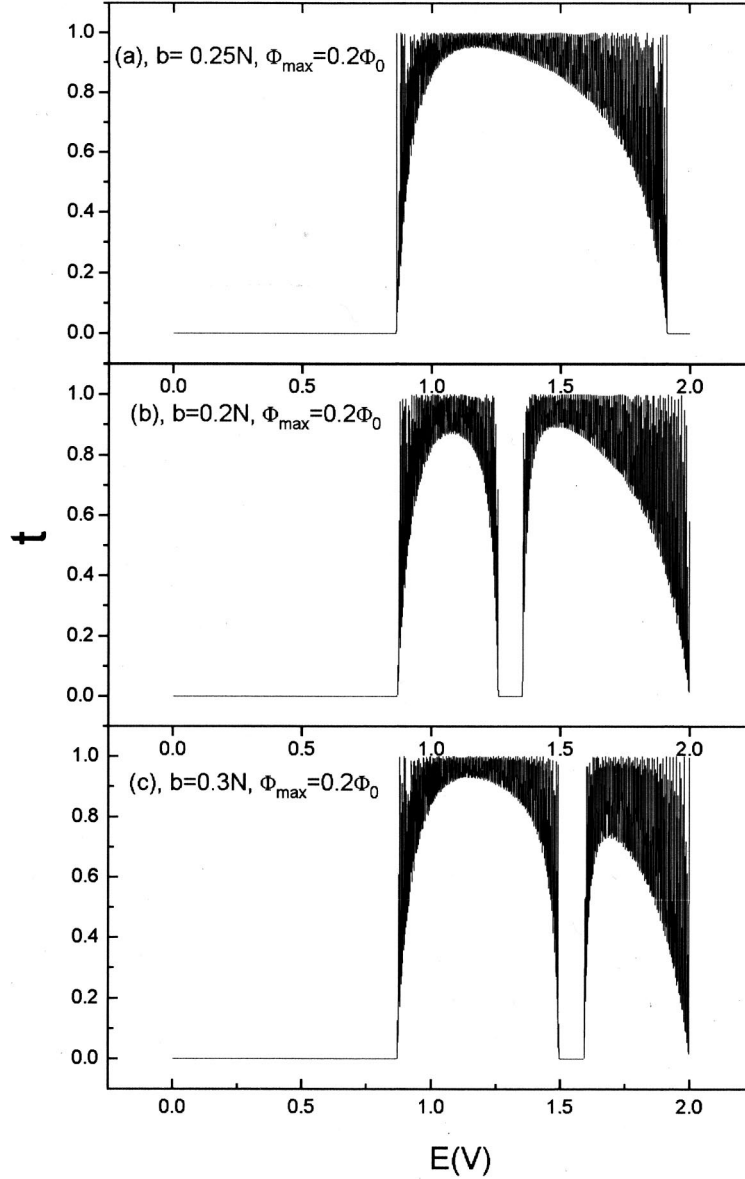


FIG. 2. The transmission coefficient as a function of energy for the case with cos-modulated flux, with different modulation period.

$$E\chi_n = e^{-i\gamma_{n-1}/4}\varphi_n + e^{i\gamma_n/4}\varphi_{n+1}, \quad (3)$$

$$E\psi_n = e^{i\gamma_{n-1}/4}\varphi_{n-1} + e^{-i\gamma_n/4}\varphi_{n+1}, \quad (4)$$

where $\gamma_i = 2\pi\Phi_i/\Phi_0$, $\Phi_0 = h/e$, and Φ_i is the flux threading i th ring of the system.

Eliminating χ_n and ψ_n leads to the following equation:

$$\left(E - \frac{4}{E}\right)\varphi_n - \frac{2}{E}\cos\frac{\gamma_{n-1}}{2}\varphi_{n-1} - \frac{2}{E}\cos\frac{\gamma_n}{2}\varphi_{n+1} = 0, \quad (5)$$

while it is a little different at the boundaries

$$\left(E - \frac{2}{E}\right)\varphi_n = \varphi_{N+1} + \frac{2}{E}\cos\frac{\gamma_{N-1}}{2}\varphi_{N-1}, \quad (6)$$

$$\left(E - \frac{2}{E}\right)\varphi_1 = \varphi_0 + \frac{2}{E}\cos\frac{\gamma_1}{2}\varphi_2. \quad (7)$$

II. MODEL

We will solve the transmission problem in the necklace system connected to the two semi-infinite linear leads. The wave function in the linear lead is taken as a single Bloch wave specified by a wave vector k . Thus

$$\varphi_n = Re^{ikn} + R_1e^{-ikn}, \quad n \leq 1,$$

$$\left(E - \frac{4}{E}\right)\varphi_n = \frac{2}{E}\cos\frac{\gamma_{n-1}}{2}\varphi_{n-1} + \frac{2}{E}\cos\frac{\gamma_n}{2}\varphi_{n+1}, \quad 1 \leq n \leq N, \quad (8)$$

$$\varphi_n = Te^{ikn}, \quad n \geq N+1,$$

where T is the transmitted amplitude; R and R_1 is the input and reflected amplitude, respectively. In the linear lead, the dispersion relation $E = 2\cos k$ holds. Thus the transmission coefficient t is

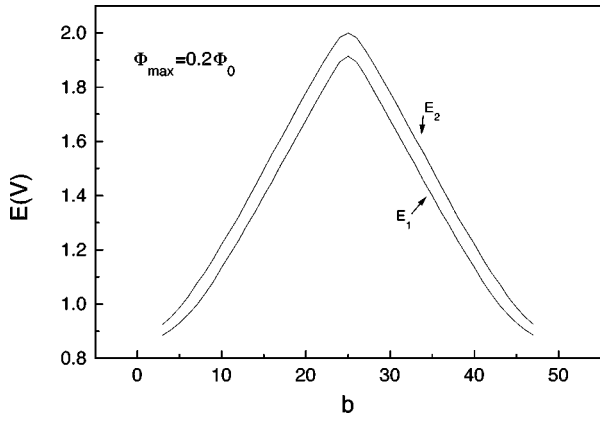


FIG. 3. The critical energy of the two subintervals as a function of modulation period (for cos-modulated flux) at fixed Φ_{max} .

$$t = \frac{|T|^2}{|R|^2}. \tag{9}$$

Without loss of generality, we set T to be 1 since in linear systems the output intensity is proportional to the input intensity.

Equation (5) can be rewritten as

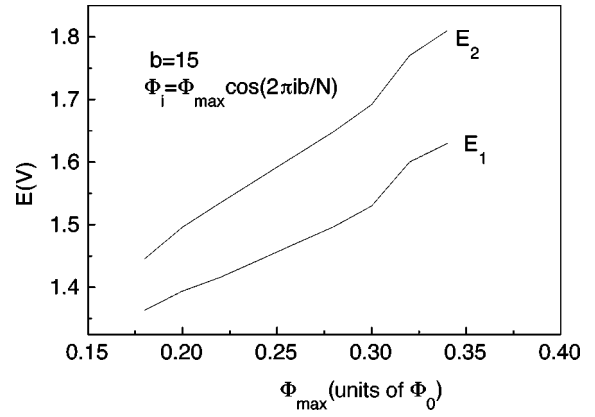


FIG. 4. The critical energy of E_1 , E_2 as a function of Φ_{max} at fixed b .

$$\begin{pmatrix} \varphi_{n+1} \\ \varphi_n \end{pmatrix} = \begin{pmatrix} \frac{E^2 - 4}{2 \cos \frac{\gamma_n}{2}} & \cos \frac{\gamma_{n-1}}{2} \\ 1 & \cos \frac{\gamma_n}{2} \end{pmatrix} \begin{pmatrix} \varphi_n \\ \varphi_{n-1} \end{pmatrix}, \tag{10}$$

introducing

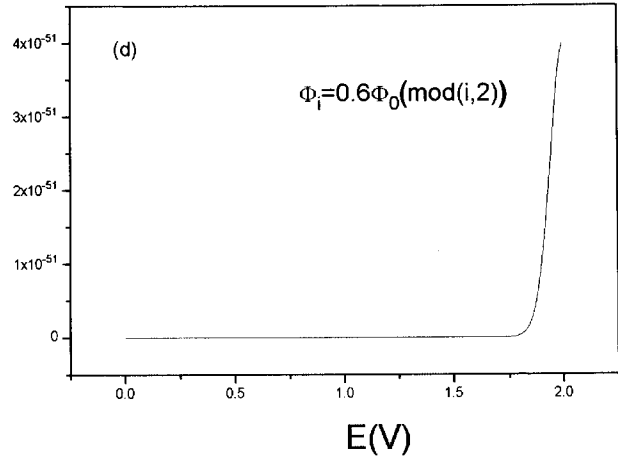
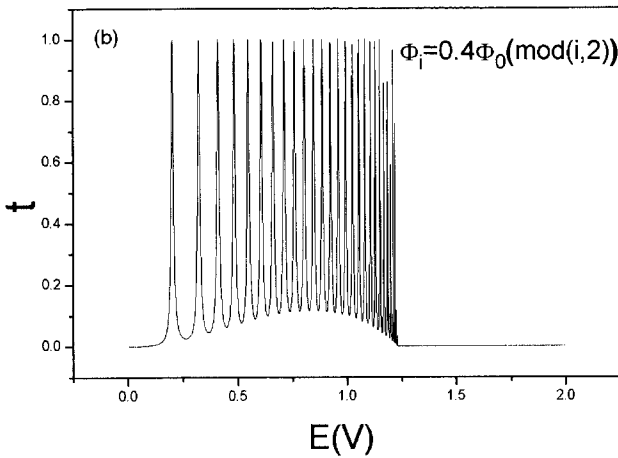
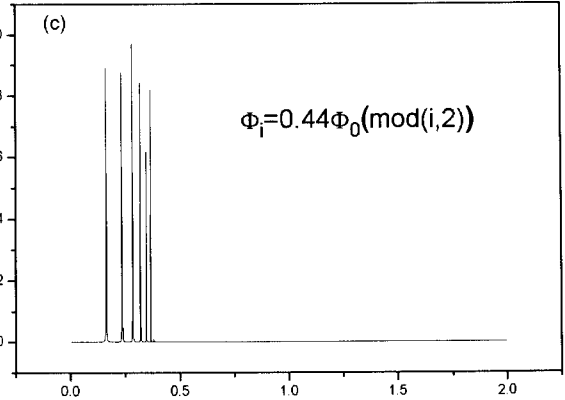
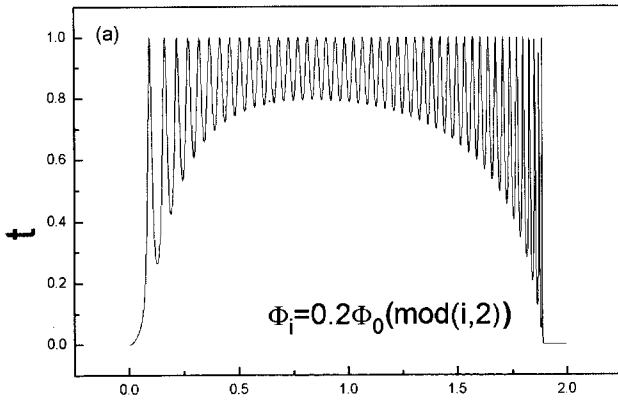


FIG. 5. The transmission coefficient as a function of energy for the case with sawtoothed flux. $l=2$. Note that for large flux no transmission is permitted.

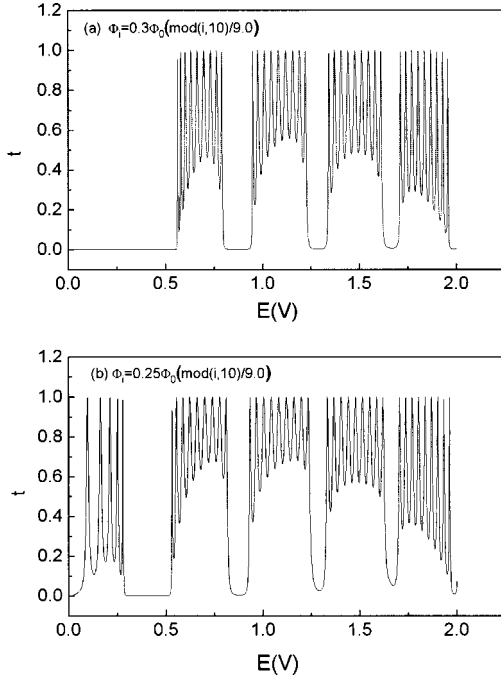


FIG. 6. The transmission as a function of energy for the case with sawtoothed flux with different modulation period.

$$M(n) = \begin{pmatrix} \frac{E^2 - 4}{2 \cos \frac{\gamma_n}{2}} & \cos \frac{\gamma_{n-1}}{2} \\ 2 \cos \frac{\gamma_n}{2} & -\cos \frac{\gamma_n}{2} \\ 1 & 0 \end{pmatrix}, \quad \Psi_{n+1} = \begin{pmatrix} \varphi_{n+1} \\ \varphi_n \end{pmatrix}, \quad (11)$$

where $M(n)$ is the transfer matrix. We can write

$$\Psi_{n+1} = M(n)\Psi_n = \dots = P(n)\Psi_1, \quad (12)$$

where $P(n) = \prod_i M(i) = M(n)M(n-1) \dots M(1)$ is the total transfer matrix. And thus the transmission coefficient is given by

$$t = \frac{4(\sin k)^2}{|[P(n)]_{21} + [P(n)]_{12} + [P(n)]_{22}e^{ik} - [P(n)]_{11}e^{-ik}|^2}. \quad (13)$$

III. RESULTS AND DISCUSSION

In the following discussion, we consider different configurations of inhomogeneous flux, and deal with only the case of the electrons with positive energy.

Considering the following modulated flux:

$$\Phi_i = \Phi_{max} \cos\left(2\pi i \frac{b}{N}\right), \quad (14)$$

where Φ_i denotes the flux threading i th loop, N is the number of loops, and b is a parameter determining the period of

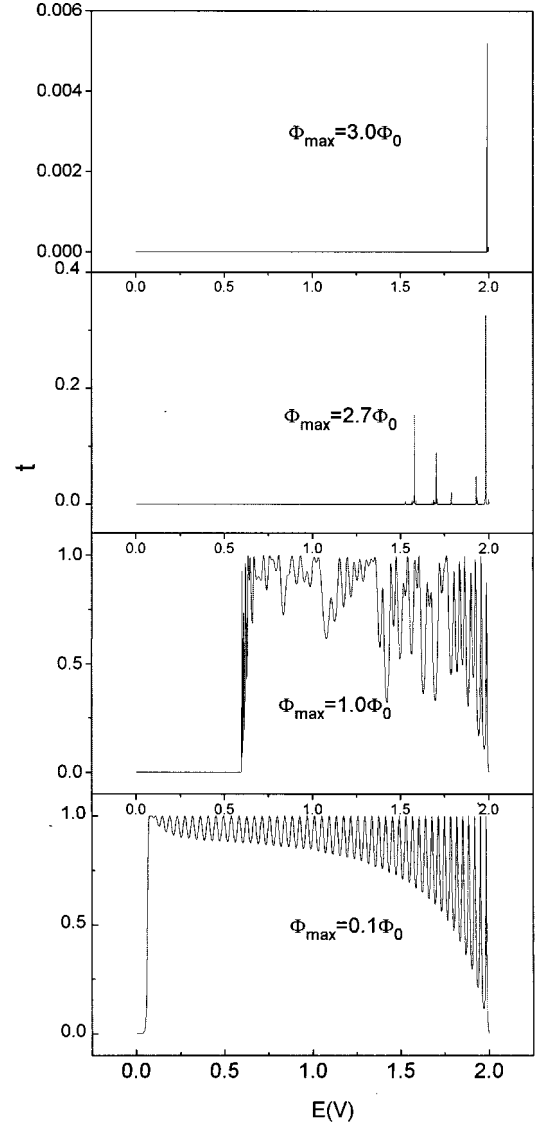


FIG. 7. The transmission of the system with random distributed flux. When the amplitude of the flux increases, the pass-bandwidth decreases.

flux. In our investigation, we take $N=100$, but the results hold for system with any even loops.

We show in Fig. 2 the main results. Numerical studies show that when $b = (k/4)N$, where $k=0, \pm 1, \pm 2, \pm 3, \dots$, transmission always occurs when the energy of the electrons is greater than a critical value E_c , as shown in Fig. 2(a). The value of E_c depends on Φ_{max} . This result is similar to the case with constant magnetic flux [20]. This can be understood if we look at Fig. 9, in which the energy spectrum of the system does not split into two (or more) subbands and there is no energy gap appearing in the case under consideration (modulated period $b = (k/4)N$), while if b is an integer other than the above values, as shown in Figs. 2(b) and 2(c), an interesting phenomenon occurs. Now transmission only occurs in the separate intervals $(E_c, E_1), (E_2, 2)$ where E_1, E_2 take different values. Studies also show that E_c is independent of b , and the values of E_1 and E_2 are related to Φ_{max} and b . This happens because of the previously mentioned phase mismatch. When the mismatch attains specific

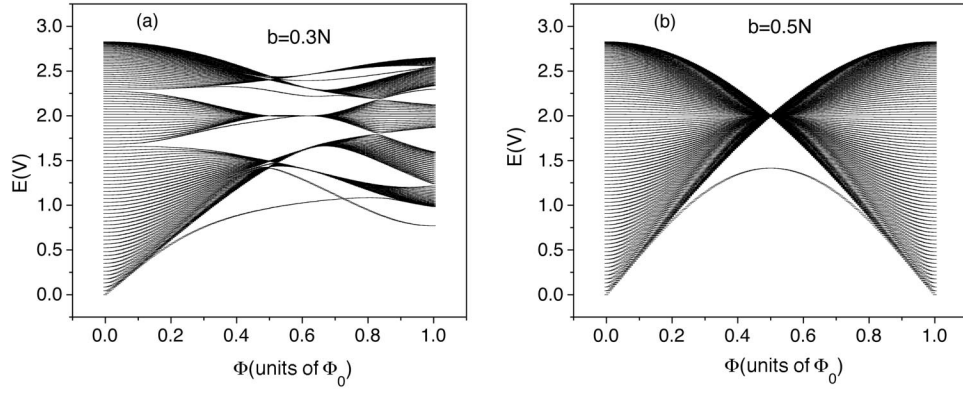


FIG. 8. The energy spectrum of the system with cos-type modulated flux as a function of flux at fixed modulation period.

values, the electrons with energy in the corresponding ranges cannot transmit through the system, thus leading to the formation of a transmission gap. This is the quantum interference effect. In order to see clearly how they change with the change of b for fixed Φ_{max} , we plot in Fig. 3 the values of E_1 and E_2 as a function of b . From the figure we can see that the increase (decrease) of E_1 and E_2 are near synchronous perfectly with the change of b thus keeping the width of the transmission gap nearly constant. In Fig. 4, for comparison, we show the change of E_1, E_2 with the change of Φ_{max} at fixed b , and they increase (decrease) “synchronously” too.

Another case we consider here is the modulated flux in the form

$$\Phi_i = \Phi_{max} \frac{\text{mod}(i, l)}{l-1}, \quad (15)$$

where l is a parameter controlling the period of the modulated flux, and i means the i th ring. It is clear that there will be l possible values of the magnetic flux. Numerical studies show that the transmission behavior in this case is much more complicated.

We will represent here the results when l takes some special values. Figure 5 corresponds to the results for the case of $l=2$, i.e., the flux in the *even* (*odd*) loop is 0 (Φ_{max}). Transmission occurs in a range (E_1, E_2) , where E_2 is a critical value less than 2, the band edge of the linear lead. The system acts as a “low-pass” filter in energy and this pass band-

width decreases with the increase of applied field until the pass band disappear if the applied flux is large enough, which can be clearly seen from the figures. As the amplitude Φ_{max} is increased to a critical value $0.445\Phi_0$, the transmission will no longer occur for even larger Φ_{max} . It is very interesting to note the blocking of electrons without any *disorder* in the case of large enough flux. This is caused exclusively by the quantum interference effect.

We show in Fig. 6 the results with $l=10$. More separate transmission gaps are exhibited. Studies show that when $\Phi_{max} \geq 0.18\Phi_0$, the energy region of the system corresponding to the whole energy band of the linear lead has been broken into several (more than two) transmission subblocks. When $\Phi_{max} \leq 0.18\Phi_0$, the transmission will always occur for the whole energy band of the linear lead, there only exist some small tips in the transmission spectra but the transmission region does not break into subblocks, which is not shown in the figure. For other l , we found even more transmission subblocks.

For comparison, we have also investigated the effects of random distributed flux. The flux considered here is chosen to be a continuous distributed random variable, and the results are shown in Fig. 7. For small amplitude of flux, most of the states can transport through the system, the effect of small disorder is not so obvious; as the amplitude of the flux increases, fewer and fewer electrons can transport through the system. These do coincide with previous results of Fig. 5. When the amplitude of the flux exceeds a critical value, no transmission occurs. In this case, disorder has played a important role. It seems that there exists a transition something like the extended-localization transition.

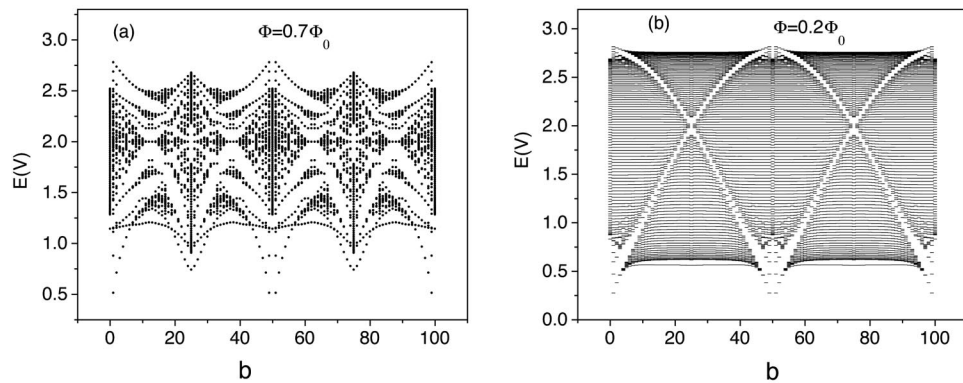


FIG. 9. The energy spectrum of the system with cos-modulated flux as a function of modulation period at fixed magnetic flux amplitude.

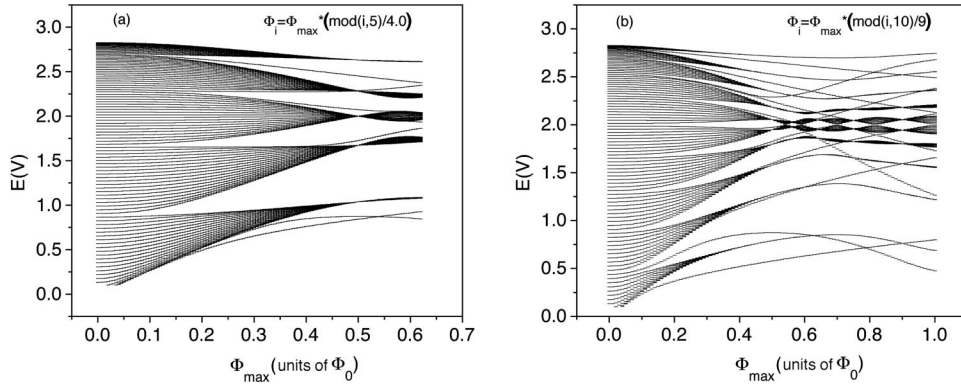


FIG. 10. The energy spectrum of the system with sawtoothed flux as a function of Φ_{max} .

In order to get insight into the above stated results, let us inspect the energy spectrum of the necklace system (excluding the linear leads at the two ends). We hereby give some of the energy spectra with different parameters in Figs. 8–10 (we have represented in the figures only the positive energy part of the corresponding energy spectrum). Figure 8(a) corresponds to a cos-modulated flux with $b=0.3N$. When the magnitude of flux is very small, the conduction band exists throughout the whole band of linear lead (0, 2), which is included in this energy spectrum, corresponding to a continuous transmission; with the increase of flux, the energy interval (0, 2) (since only the electrons with energy less than 2 can propagate through the lead) splits into two subbands separated by a gap between them, which contributes to the transmission gap in the previous figure. In Fig. 8(b), the case of $b=0.5N$, we find a rather different energy spectrum. It does not split with the increase of applied flux, thus leading to a continuous transmission spectra when the energy of incident electron is greater than a critical value. This can be clearly seen from Eqs. (5) and (8). For this modulation period, the “cos” term in the equation is the same for two succeeding rings, thus it is just the same as the constant flux case. In this case, the energy spectrum can be written in a closed form [20]:

$$E = \pm 2 \sqrt{1 + \cos \frac{\gamma}{2} \cos k}, \quad (16)$$

when γ is π , E is equal to ± 2 , and consequently no electrons can transport through the system.

In Fig. 9 we show the energy spectra (for cos-type modulation) as a function of modulation period at different Φ_{max} . Figure 9(a) is the case with a relatively greater flux. The energy spectra show a complicated pattern, corresponding to a complicated transmission behavior. Figure 9(b) is the case with a relatively smaller flux. It is clear that a gap occurs in the energy spectra, corresponding to the transmission gap between the two transmission intervals in Fig. 3, and the two permitted energy bands corresponding to the transmission zone in Fig. 3. We can also find that when $b=0.25kN$ (where k is an integer), the energy spectrum within (0,2) doesn’t split, indicating a continuous transmission in the interval $(E_c, 2)$.

The energy band of the system with sawtooth modulated has also been investigated in the case of two different periods and the results are shown in Fig. 10. Figure 10(a) is the case with $l=5$. Now the energy spectra is to some extent similar to the case with cos-modulated flux, but the energy spectra splits into more subbands than the latter case. Figure 10(b) is the case of $l=10$; clearly, even more subbands occur. In both of the above cases, with the increase of flux the conduction bands become increasingly narrow, the gaps become increasingly wide; and the separated conduction bands even overlap if the flux is large enough.

IV. SUMMARY

We have investigated the quantum interference effects on transmission properties of the necklace loop structure with modulated flux and many interesting results have been obtained. For periodic modulated flux, the transmission properties of electrons are sensitive to both the modulation mode and amplitude. We found interesting on-off phenomena in the transmission spectra, which may be useful in fabricating special devices. As a physical application, for example, by controlling the period or the amplitude of the flux we can select the electrons with the required energy to transport through the system, thus used as a energy “filter,” or a switch, etc. As to the experimental realization of this system: first, people can fabricate this structure without any difficulty with the development of modern nanotechnology; second, the inhomogenous magnetic field can be realized as follows the necklace system can be placed on a substrate that is threaded with a homogenous magnetic field, and the susceptibility of the substrate can vary on the scale of the size of a single ring, with a mode of the required modulation. The magnetic flux can also be detected with already existing device such as a SQUID microscope. For disordered flux, with the increase of the amplitude of flux, fewer and fewer electrons can transport through the system, until the amplitude of the flux exceeds a critical value after which no transmission can occur.

For an explanation from other aspects of the physics of the transmission problem, we have calculated the energy spectra of the system as a function of the amplitude and modulation period of the flux and found that the transmission properties can be understood from the energy band.

- [1] *Mesoscopic Phenomena in Solids*, edited by B. L. Altshuler, P. A. Lee, and R. A. Webb (North-Holland, New York, 1991).
- [2] *Transport Phenomena in Mesoscopic Systems*, edited by H. Fukuyama and T. Ando (Springer-Verlag, Berlin, 1992).
- [3] R. Landauer, *Philos. Mag.* **21**, 863 (1970).
- [4] H. L. Engquist and P. W. Anderson, *Phys. Rev. B* **24**, 1151 (1981).
- [5] M. Buttiker, Y. Imry, and R. Landauer, *Phys. Lett.* **96A**, 365 (1983).
- [6] Y. Gefen, Y. Imry, and M. Ya. Azbel, *Phys. Rev. Lett.* **52**, 129 (1984).
- [7] M. Buttiker, Y. Imry, R. Landauer and S. Pinhas, *Phys. Rev. B* **31**, 6207 (1985).
- [8] U. Sivan and Y. Imry, *Phys. Rev. B* **33**, 551 (1986).
- [9] O. Entin-Wohlman, C. Hartzstein, and Y. Imry, *Phys. Rev. B* **34**, 921 (1986).
- [10] L. P. Levy, G. Dolan, J. Dunsmuir, and H. Bouchiat, *Phys. Rev. Lett.* **64**, 2074 (1990).
- [11] Wenji Deng, Youyan Liu, and Changde Gong, *Phys. Rev. B* **50**, 7655 (1994).
- [12] D. Kowal, U. Sivan, O. Entin-Wohlman, and Y. Imry, *Phys. Rev. B* **42**, 9009 (1990).
- [13] Youyan Liu, Honglin Wang, Zhaoqing Zhang, and Xiujun Fu, *Phys. Rev. B* **53**, 6943 (1996).
- [14] J. Xia, *Phys. Rev. B* **45**, 3593 (1992).
- [15] D. Takai and K. Ohta, *Phys. Rev.* **51**, 11 132 (1995).
- [16] Yan Chen, Shijie Xiong, and S. N. Evangelou, *Phys. Rev. B* **56**, 4778 (1997).
- [17] Daisuke Takai and Kuniichi Ohta, *Phys. Rev. B* **50**, 2685 (1994).
- [18] Daisuke Takai and Kuniichi Ohta, *Phys. Rev. B* **50**, 18 250 (1994).
- [19] B. Doucot, R. Rammal, *J. Phys. (Paris)* **47**, 973 (1986).
- [20] Zhiwen Pan, Shijie Xiong, and Changde Gong, *Phys. Rev. E* **58**, 2408 (1998).